

Facile Inkjet-Printing Self-Aligned Electrodes for Organic Thin-Film Transistor Arrays with Small and Uniform Channel Length

Jason Doggart,^{†,‡} Yiliang Wu,^{*,§} Ping Liu,[§] and Shiping Zhu^{*,‡}

Materials Synthesis & Characterization Laboratory, Xerox Research Centre of Canada, Mississauga, Ontario, Canada L5K 2L1, and Department of Chemical Engineering, McMaster University, Hamilton, Ontario, Canada L8S 4L8

ABSTRACT We demonstrated a facile method for fabrication of source and drain electrodes with very reproducible narrow channel length without any intermediate processing steps. Organoamine-stabilized silver nanoparticles ink enables in situ formation of a hydrophobic boundary around the first printed electrodes, which repels subsequently deposited ink to a consistent distance. Because of this self-alignment nature, small printing errors could be automatically corrected, allowing for large defect-free source drain arrays to be printed with a very narrow distribution of channel length. Furthermore, electrodes printed with this method were used to fabricate OTFT array, showing high yield, high mobility, and on/off ratio.

KEYWORDS: inkjet printing • organic thin-film transistor • self-alignment • silver nanoparticles

Printed organic thin film transistors (OTFTs) have recently shown tremendous promise for use in low-end or disposable electronics such as RFID tags, sensors, or liquid crystal displays (1–5). These OTFTs promise to drastically reduce fabrication costs because of their low energy requirements, minimal capital investment, and process simplification. Furthermore, these devices require processing temperatures of less than 150 °C, allowing for fabrication on lightweight flexible substrates (6–12). Inkjet printing has been shown to have great potential as a method of fabrication for these devices because of its ability to print multiple components on a layer-by-layer basis with the potential for very high resolution (2, 13–21). In fact, some groups have already demonstrated the fabrication of inkjet printed high-performance OTFTs (4, 5, 18, 21). Unfortunately, all of these demonstrations have required intermediate processing steps that drive up the fabrication cost because of increased fabrication complexity.

One of the reasons for these undesired intermediate processing steps is the requirement of the source and drain electrodes being printed such that they are very close to each other, giving a very small channel length. Unfortunately, as the channel length is decreased, the probability of device failure increases significantly. This is due to shorting between the electrodes which occurs because of splashing and spreading of droplets impacting the substrate. Therefore, when no intermediate processing steps are used, the resolution is usually limited to printing devices with channel

lengths of 50–100 μm . Various methods have been suggested to print small and uniform channel lengths for OTFTs. Some group has obtained channel lengths of 1–10 μm either by reducing the volume of the ink droplet with very fine nozzles such as subfemtoliter inkjet printing and electrohydrodynamic jet printing (13, 14), or by printing a single electrode then laser ablating a channel (6). Other groups have demonstrated very narrow channels by pre patterning the substrate with hydrophobic regions (5, 20). Although these methods are effective, they are costly, complex, and time-consuming. As an alternative, Siringhaus et al. have demonstrated a self-alignment technique that can be used to obtain sub micrometer channel lengths. In this technique, a single electrode is printed and surface-modified with a fluorinated monolayer. When a second electrode is printed such that it slightly overlaps the first, the low surface energy of the modified original electrode causes it to dewet from the surface, forming a very narrow gap (4). Although this method is simpler than others, it still requires an undesirable intermediate processing step for the modification.

Here, we demonstrate a facile self-alignment technique for fabricating source and drain electrodes in OTFT devices that requires no intermediate processing steps and results in very reproducible channel lengths as low as 10 μm . This method uses a hydrophobic boundary around the first printed electrodes on a hydrophilic substrate, which is formed during the printing process. Ink subsequently printed in the vicinity of the original electrode is repelled by this boundary creating a narrow channel. Furthermore, this self-alignment method automatically compensates for small printing errors or irregularities in the original printed electrode allowing for transistor arrays to be printed with not only very narrow channel length distribution but also high device yield. This could be particularly interesting for the development of a complete roll-to-roll fabrication process.

* To whom correspondence should be addressed. E-mail: Yiliang.Wu@Xerox.com (Y.W.); zhuship@mcmaster.ca (S.Z.).

Received for review May 27, 2010 and accepted August 1, 2010

[†] Visiting student at Xerox Research Centre of Canada.

[‡] McMaster University.

[§] Xerox Research Centre of Canada.

DOI: 10.1021/am100466r

2010 American Chemical Society

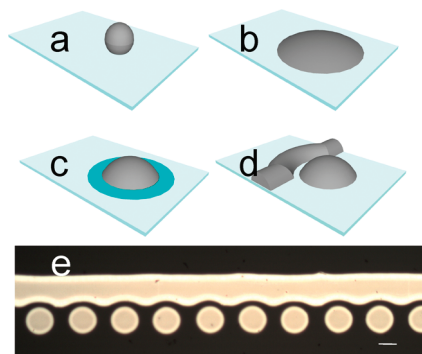


FIGURE 1. Schematic illustrating the method used for self-alignment. Droplets ejected from the inkjet printer (a) impact the surface and (b) spread to a maximum radius R_m . (c) The surface tension of the ink and the surface energy of the substrate then cause the ink to recede to some final radius R_f during which organoamine is deposited on the substrate (light blue region). (d) Subsequent ink deposited in the proximity of the original feature is repelled by the hydrophobic boundary layer. (e) This repulsion is evident in the optical microscope image, where the dots array was printed first, followed by a line printed close to the dots array. The scale bar represents $50\ \mu\text{m}$.

Our method takes advantage of the dynamics of a droplet impacting a solid surface during printing. Upon impact, the kinetic energy contained within the droplet drives it to spread to some maximum radius R_m after which the surface tension of the ink and the surface energy of the substrate drive the droplet to recede to some final radius, R_f (22). We hypothesized that it may be possible to include a surface modification agent in the ink that would modify a hydrophilic substrate during this spreading, resulting in a hydrophobic boundary surrounding any printed feature. This hydrophobic boundary would then repel any ink subsequently deposited in the proximity of the original printed feature because of surface energy contrast between the relatively hydrophobic boundary and the hydrophilic substrate, resulting in a self-aligned channel. A schematic of this method is illustrated in Figure 1a–d.

To demonstrate this concept, a silver nanoparticle ink developed at the Xerox Research Center of Canada was used. Silver nanoparticles with an average diameter of 5 nm were synthesized by reduction of silver acetate in the presence of organoamine such as hexadecylamine as the stabilizer (10). These silver nanoparticles were dispersed in a mixture of dodecane and terpineol, where dodecane is a good solvent for the silver nanoparticles. It is known that stabilizer desorption takes place readily in good solvents, which has been utilized for stabilizer exchange and digestive ripening for nanoparticle synthesis (23, 24). In the ink formulation, when a polar solvent terpineol was added, which is a good solvent for hexadecylamine, an equilibrium was reached between hexadecylamine adhered to the silver nanoparticles and free (desorbed) hexadecylamine. This was clearly shown by differential scanning calorimetry (DSC) measurement of the reprecipitated silver nanoparticles of the ink, where the melting peaks of hexadecylamine were detected (see Figure S1 in the Supporting Information). Free hexadecylamine stabilizer is able to adhere to the plasma cleaned glass, which drastically reduces its surface energy. To demonstrate this,

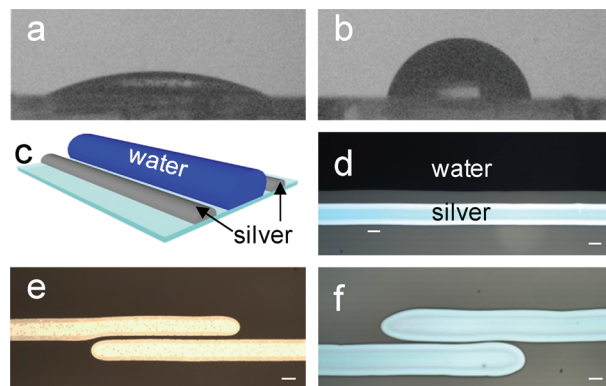


FIGURE 2. Water contact angle of (a) plasma cleaned glass was shown to increase from 25 to 78° when (b) the surface was modified with hexadecylamine. (c) To show that free organoamine within the silver nanoparticle ink also modified the substrate surface, two lines were printed $5\ \text{mm}$ apart and $4\ \mu\text{L}$ of water was dropped between them. It is evident from (d) the optical microscope image that a $50\ \mu\text{m}$ hydrophobic boundary existed around the printed silver. When overlapping silver electrodes were printed on plasma cleaned glass, the hydrophobic boundary caused the second electrode to be repelled, (e) creating a narrow channel seen in the optical image. When the same two electrodes were printed on hexadecylamine modified glass, (f) no repulsion was seen in the optical image. The scale-bars represent $50\ \mu\text{m}$.

we dip-coated air plasma cleaned glass with a 3 wt % hexadecylamine solution in toluene and allowed it to dry. As shown in images a and b in Figure 2, the water contact angle on the modified substrate was significantly higher than that on the plasma cleaned glass (78.3 and 25° , respectively) confirming that hexadecylamine was indeed able to lower the surface energy of the glass. Similarly, the silver nanoparticle ink wetted the plasma cleaned substrate very well—it spread quickly and resulted in a very low contact angle; on the other hand, the ink showed a much higher contact angle and spread much less on hexadecylamine modified glass substrate (see Figure S2 in the Supporting Information). We therefore utilize the free (desorbed) hexadecylamine in the ink as the surface modification agent to create a hydrophobic boundary around the printed features during the printing process. This in situ modification of the substrate surface around the first printed feature resulted in substrate surface energy difference, and thus the wetting and spreading difference of the subsequently deposited ink. As a result, a self-aligned channel would be formed.

The ability of organoamine to create a low surface energy boundary around electrodes through the inkjet printing process was further demonstrated by printing two silver lines $5\ \text{mm}$ apart, followed by a $4\ \mu\text{L}$ droplet of water placed between the lines. The water spread easily on the plasma cleaned glass between the lines but was held a distance of $50\ \mu\text{m}$ away from the printed lines. This confirmed that a hydrophobic boundary around the electrode was indeed created during the printing process. This can be seen schematically in Figure 2c and in an image taken from an optical microscope in Figure 2d.

Having shown that our method effectively creates a hydrophobic boundary surrounding the printed silver nanoparticle features, we then sought to demonstrate that this could be useful for fabrication of source and drain electrodes

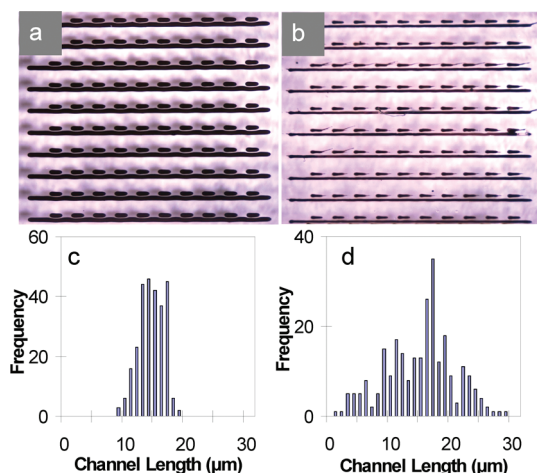


FIGURE 3. Optical microscope images of 10×10 transistor arrays printed using (a) our new silver nanoparticle ink and (b) a commercial ink. Histograms showing distribution of channel lengths for transistors printed with (c) our new silver nanoparticle ink and (d) commercial ink.

with very small and uniform channel length. As shown in Figure 1e, a dot array was printed, followed by a line close to the dots. The edge of the line facing the dots bent nicely around the dots array to form small and uniform gaps, whereas the other edge of the line was very smooth. To further demonstrate printing transistor channel, two lines were printed such that their ends overlap for $500 \mu\text{m}$. It is evident in Figure 2e that the second line was clearly repelled by the first line, resulting in a very narrow ($12 \mu\text{m}$) channel. This result was found to be consistent and reproducible. To demonstrate that this self-alignment was indeed caused by surface energy contrast between the selectively modified area by hexadecylamine and the nonmodified area, the same pattern was printed on glass substrates, which had been previously modified with hexadecylamine. As can be seen in Figure 2f, no self-alignment behavior was observed in this case, because there was no surface energy contrast during the printing process.

Ten-by-ten arrays of source and drain electrodes were then printed using this new ink formulation with self-alignment capability, and a commercial ink (ANP, DGP-40LT-15C) containing no surface modification agent was used as a control experiment for comparison. For demonstration, simple source/drain arrays as shown in images a and b in Figure 3 were printed (18), wherein a row of transistors has a common source electrode and separated drain electrode. The channel lengths of the 100 transistors in these arrays were measured at three locations for each transistor. These measurements were plotted as histograms, shown in panels c and d in Figure 3. It is clear that the arrays printed using our new ink formulation showed greatly reduced channel length distribution. This is due to the self-correcting attributes associated with the self-alignment technique. Mis-fired droplets that occurred during printing had little influence because the subsequent printed features self-aligned at a constant distance away from them, allowing for a consistent channel length in spite of printing errors. We therefore achieve 100% device yield without shorting be-

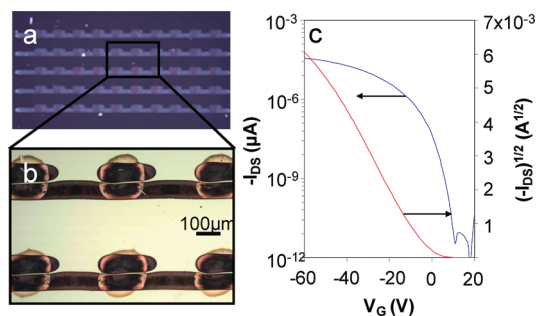


FIGURE 4. (a) A 10×5 OTFT array fabricated using inkjet printed silver source and drain electrodes and inkjet printed PQT-12 semiconductor. (b) When magnified one can see the narrow and consistent channel achieved using this printing method. (c) Drain current vs gate voltage in saturation regime ($V_D = -60 \text{ V}$) for a device fabricated on OTS-8 modified substrate. Devices fabricated in this manner showed very high mobility and on/off ratio.

tween the source drain electrodes. On the other hand, the array printed using the commercial ink without the self-correction capability showed large channel length variation and shorting between source and drain electrodes in some transistors. To our best practice, we were able to achieve only 85% device yield.

For this method to be useful for OTFT application, it is necessary that the organoamine within the channel not detract from the device performance. To investigate this, we fabricated OTFT arrays using this new method for inkjet printing source and drain electrodes (Figure 4). These electrodes were printed onto heavily doped n-type silicon (gate) with a 200 nm SiO_2 layer (dielectric). After annealing the printed silver nanoparticle electrodes at $140 \text{ }^\circ\text{C}$, a temperature compatible with plastic substrate, we inkjet printed poly(3,3'-didodecylquater-thiophene) (PQT-12) into the channel. All transistors functioned well without shorting between source and drain electrodes. Interestingly, the transistors exhibited an average mobility of $0.02 \text{ cm}^2/(\text{V s})$ with the bare silicon oxide dielectric. Previous reports have shown the mobility of devices fabricated on unmodified SiO_2 to be $0.0004 \text{ cm}^2/(\text{V s})$ (25), indicating that our process improves the device performance by nearly 2 orders of magnitude. This is probably due to the effect of in situ modifying the channel region with the hexadecylamine. It has been shown that octanethiol modification of gold source drain electrodes helped reduce contact resistance and that octyltrichlorosilane (OTS-8) was the best choice for the dielectric surface modification (9, 25). We therefore plasma treated the silicon wafer after source drain fabrication (to remove the organoamine stabilizer) then modified the dielectric with OTS-8 and the silver electrode with octanethiol. The mobility was further improved to an average of $0.07 \text{ cm}^2/(\text{V s})$ with some devices showing mobility as high as $0.1 \text{ cm}^2/(\text{V s})$ and on/off ratios of 1×10^6 , which are in line with the best inkjet printed PQT-12 transistors (18, 21).

Our work has demonstrated a facile method for fabrication of source and drain electrodes with very reproducible narrow channel length without the need for any intermediate processing steps. The use of organoamine as a stabilizer for silver nanoparticles allows a hydrophobic boundary around electrodes to be formed during the printing process.

This boundary repels subsequently deposited ink to a consistent distance from the original electrode. Since this method relies on self-alignment, it is also able to automatically compensate for small printing errors, allowing for large defect-free source drain arrays to be printed with a very narrow distribution of channel length. Furthermore, we have demonstrated that electrodes fabricated with this method can be used to fabricate OTFT devices with very high mobility and on/off ratio. Integration of this fabrication method for source and drain electrodes together with printable dielectric materials for all printed transistor arrays is underway. We believe that our method would be very useful for the development of all printed low-cost OTFT devices.

EXPERIMENTAL SECTION

Hexadecylamine-stabilized silver nanoparticles were synthesized according to previously published method (10). Silver nanoparticle ink was formulated by mixing 2 parts silver nanoparticles with 2 parts dodecane and 1 part terpeneol by weight.

Glass substrates used for printing were washed using IPA, plasma cleaned for 3 min under air, rinsed with deionized water and IPA, and then dried with compressed and filtered air. Some substrates were then modified further by first dip coating in a 3 wt % solution of hexadecylamine in toluene then drying at 60 °C for 30 s.

To avoid device failure from dielectric, we chose to build our OTFT devices on heavily doped silicon wafer with a 200 nm thermally grown SiO₂ layer as the gate dielectric. This reliable dielectric enables us to evaluate the device yield from source/drain shorting only. The wafer substrate was cleaned in the same manner as the glass substrate. The silver nanoparticle ink was printed into fine lines as source and drain electrodes with a Dimatix DMP 2800 drop-on-demand inkjet printer equipped with a 10 pL print head at a substrate temperature of 60 °C. Drop velocity was set to 5 m/s by controlling the nozzle voltage. The printed silver nanoparticle features were then annealed at 140 °C under atmospheric conditions for 10 min to obtain highly conductive silver electrodes.

After printing and annealing, some substrates were air plasma cleaned for 2 min, then modified with a 1 wt % solution of octyltrichlorosilane (OTS-8) in toluene by spin coating for 20 s. These substrates were allowed to dry at 60 °C, were further modified with a 1 wt % solution of octanethiol in toluene by spin coating for 20 s.

A PQT-12 solution was printed into the channel of these source and drain electrodes using the same printer as above. In this case, the substrate was kept at room temperature during printing. After printing the device was annealed in a vacuum oven at 140 °C for 10 min to enhance the performance of the semiconductor. The OTFTs were characterized using Keithley SCS 4200 system with a three-point probe station under ambient conditions, using the sharp probe to contact the common source electrode and separated drain electrodes for each transistor individually.

Supporting Information Available: DSC traces for hexadecylamine-stabilized silver nanoparticles and hexadecylamine; contact angle measurements for silver nanoparticle ink on modified and non-modified substrates (PDF). This material is available free of charge via the Internet at <http://pubs.acs.org>.

REFERENCES AND NOTES

- (1) Yang, L.; Rida, A.; Vyas, R.; Tentzeris, M. M. *IEEE Trans. Microwave Theory Tech.* **2007**, *55*, 2894.
- (2) Noguchi, Y.; Sekitani, T.; Someya, T. *Appl. Phys. Lett.* **2006**, *89*, 253507.
- (3) Rogers, J. A.; Bao, Z.; Baldwin, K.; Dodabalapur, A.; Crone, B.; Raju, V. R.; Juck, V.; Katz, H.; Amundson, K.; Ewing, J.; Drzaic, P. *Proc. Natl. Acad. Sci.* **2001**, *98*, 4835.
- (4) Zhao, N.; Chiesa, M.; Siringhaus, H.; Li, Y.; Wu, Y.; Ong, B. *J. Appl. Phys.* **2007**, *101*, 064513.
- (5) Wang, J. Z.; Zheng, Z. H.; Li, H. W.; Huck, W. T. S.; Siringhaus, H. *Nat. Mater.* **2004**, *3*, 171.
- (6) Ko, S. H.; Chung, J.; Choi, Y.; Grigoropoulos, C. P.; Bieri, N. R.; Choi, T.; Dockendorf, C.; Poulikakos, D. *Proc. SPIE* **2005**, *97*, 5713.
- (7) Wu, Y.; Li, Y.; Ong, B. *S. J. Am. Chem. Soc.* **2007**, *129*, 1862.
- (8) Wu, Y.; Li, Y.; Ong, B. *S. J. Am. Chem. Soc.* **2006**, *128*, 4202.
- (9) Wu, Y.; Li, Y.; Liu, P.; Gardner, S.; Ong, B. *S. Chem. Mater.* **2006**, *18*, 4627.
- (10) Li, Y.; Wu, Y.; Ong, B. *S. J. Am. Chem. Soc.* **2005**, *127*, 3266.
- (11) Wu, Y.; Li, Y.; Ong, B. S.; Liu, P.; Gardner, S.; Chiang, B. *Adv. Mater.* **2005**, *17*, 184.
- (12) Pan, H.; Li, Y.; Wu, Y.; Liu, P.; Ong, B. S.; Zhu, S.; Xu, G. *J. Am. Chem. Soc.* **2007**, *129*, 4112.
- (13) Sekitani, T.; Noguchi, Y.; Zschieschang, U.; Klauk, H.; Someya, T. *Proc. Natl. Acad. Sci. U.S.A.* **2008**, *105*, 4976.
- (14) Park, J. U.; Hardy, M.; Kang, S. J.; Barton, K.; Adair, K.; Mukhopadhyay, D. K.; Lee, C. Y.; Strano, M. S.; Alleyne, A. G.; Georgiadis, J. G.; Ferreira, P. M.; Rogers, J. A. *Nat. Mater.* **2007**, *6*, 782.
- (15) Lim, J. A.; Lee, W. H.; Lee, H. S.; Lee, J. H.; Park, Y. D.; Cho, K. *Adv. Funct. Mater.* **2008**, *18*, 229.
- (16) van Osch, T. H. J.; Perelaer, J.; de Laat, A. W. M.; Schubert, U. S. *Adv. Mater.* **2008**, *20*, 343.
- (17) Kim, D.; Jeong, S.; Moon, J.; Kang, K. *Mol. Cryst. Liq. Cryst.* **2006**, *459*, 45.
- (18) Arias, A. C.; Ready, S. E.; Lujan, R.; Wong, W. S.; Paul, K. E.; Salleo, A.; Chabinc, M. L.; Apte, R.; Street, R. A.; Wu, Y.; Liu, P.; Ong, B. *Appl. Phys. Lett.* **2004**, *85*, 3304.
- (19) Kawase, T.; Shimoda, T.; Newsome, C.; Siringhaus, H.; Friend, R. H. *Thin Solid Films* **2003**, *438–439*, 279.
- (20) Siringhaus, H.; Kawase, T.; Friend, R. H.; Shimoda, T.; Inbasekaran, M.; Wu, W.; Woo, E. P. *Science* **2000**, *290*, 2123.
- (21) Paul, K. E.; Wong, W. S.; Ready, S. E.; Street, R. A. *Appl. Phys. Lett.* **2003**, *83*, 2070.
- (22) Dong, H.; Carr, W. W.; Bucknall, D. G.; Morris, J. F. *AIChE J.* **2007**, *53*, 2606.
- (23) Zhang, Q.; Xie, J.; Liang, J.; Lee, J. *Adv. Funct. Mater.* **2009**, *19*, 1387.
- (24) Hostetler, M. J.; Templeton, A. C.; Murray, R. W. *Langmuir* **1999**, *15*, 3782.
- (25) Wu, Y.; Liu, P.; Ong, B. S.; Srikumar, T.; Zhao, N.; Botton, G.; Zhu, S. *Appl. Phys. Lett.* **2005**, *86*, 142102.

AM100466R